

AMAZON RAIN FOREST CLASSIFICATION USING J-ERS-1 SAR DATA

A. Freeman, C. Kramer, M. Alves, and B. Chapman
Jet Propulsion Laboratory
California Institute of Technology
4800 Oak Grove Drive
Pasadena, CA 91109, USA

ABSTRACT

The Amazon rain forest is a region of the earth that is undergoing rapid change. Man-made disturbance, such as clear cutting for agriculture or mining, is altering the rain forest ecosystem. For many parts of the rain forest, seasonal changes from the wet to the dry season are also significant. Changes in the seasonal cycle of flooding and draining can cause significant alterations in the forest ecosystem.

Because much of the Amazon basin is regularly covered by thick clouds, optical and infrared coverage from the IANSAAT and SPOT satellites is sporadic. Imaging radar offers a much better potential for regular monitoring of changes in this region. In particular, the J-ERS-1 satellite carries an L-band HH SAR system which, via an on-board tape recorder, can collect data from almost anywhere on the globe at any time of year.

In this paper, we show how J-ERS-1 radar images can be used to accurately classify different forest types (i.e., forest, hill forest, flooded forest), disturbed areas such as clear cuts and urban areas, and river courses in the Amazon basin. J-ERS-1 data has also shown significant differences between the dry and wet season, indicating a strong potential for monitoring seasonal change. The algorithm used to classify J-ERS-1 data is a standard maximum-likelihood classifier, using the radar image local mean and standard deviation of texture as input. Rivers and clear cuts are detected using edge detection and region-growing algorithms. Since this classifier is intended to operate successfully on data taken over the entire Amazon, several options are available to enable the user to modify the algorithm to suit a particular image.

This work was performed by the Jet Propulsion Laboratory, California Institute of Technology, under contract from the National Aeronautics and Space Administration. The authors would like to express their thanks to NASDA for their support of this work and to Masanobu Shimada for providing the data.

INTRODUCTION

The J-ERS-1 satellite travels in a 570 km altitude orbit with a payload that includes an L-band, HH-polarized SAR with a 21 m X 21 m resolution, which images at incidence angles between 30 and 38 degrees [1]. The J-ERS-1 SAR is the first polar-orbiting imaging radar system capable of monitoring the whole of the Earth's land surface. Further, because of the ability of imaging radar to see through clouds and at night, the J-ERS-1 SAR is suited to multi-temporal studies of the Earth's land surface.

Unlike the European ERS-1 SAR, which was primarily designed for studying the world's ocean and ice-covered areas, the wavelength, polarization, incidence angle and sensor performance of the J-ERS-1 SAR are well-suited for studies of vegetation cover on land ([2], [3]). A look at some examples of J-ERS-1 SAR images over forested areas will soon verify this: clear-cut areas, flooded forests, marshland, and water channels can easily be separated visually.

As a first step towards using J-ERS-1 SAR data to map the vegetation cover over the whole Amazon, in 1993 we conducted a campaign in the Western Amazon at the Manu National Park in Peru. The campaign involved ground measurements and near-simultaneous overflights of J-ERS-1 and the NASA/JPL AIRSAR systems. Immediately afterward, a classifier which operated on this J-ERS-1 SAR data was created which displayed considerable promise. In order to form more representative training patterns and increase the robustness of the classifier, additional data was gathered over Brazil and incorporated into the algorithm. In this paper, we discuss an approach for automatic classification of basic vegetation types that can be identified in J-ERS-1 SAR data taken over the Western Amazon and Brazil. The parameters used as features for the classifier are radar backscatter (σ^0) and a texture measure. Several potential uses exist for this information, including surveying forest types, monitoring seasonal changes such as flooding, and tracking clear-cut areas.

THE TEST SITES

The J-ERS-1 SAR images used for classification were taken from three separate areas of the Amazon rain forest:

- (1) Manu National Park, Peru
- (2) Manaus, Brazil
- (3) Sena Madureira, Brazil.

A plant and wildlife preserve protecting areas of the Western Amazon, Manu National Park is a popular study site due to its biodiversity and pristine conditions. Manaus and Sena Madureira are also important sites studied by scientists worldwide. Data from all of these sites were compiled to form a set of training patterns for the classifier. These patterns then served as prototype vegetation models against which all J-ERS-1 images of the Amazon were compared.

All three of these test sites experience two seasons: the dry season lasting roughly from May to September and the wet spanning October to April. Looking at the same J-ERS-1 scene taken during different seasons, extensive forest flooding and the inundation of small oxbow lakes called *cochas* are readily apparent due to a strong L-band response. These obvious features can be detected and measured by our classifier.

From ground measurements and study of J-ERS-1 SAR images of Manu, two different forest patterns have been differentiated in the Western Amazon, upland forest and floodplain forest. Upland forest occurs in two varieties, the first occurring in hilly regions of Manu north of the Rio Madre de Dios. The hills are from 20-30m high and between 50-150m wide, thereby protecting much of the forest from river flooding. Hilly forests are composed of a mosaic of mature forests with a height ranging from 20-45m. On the hill tops the canopy is closed, while on the slopes and in rivulets between hills palm and bamboo becomes more prevalent. This forest type is also semi-deciduous, which implies that some tree species lose their leaves in the dry season. The second type of upland forest is found on a plateau between the base of the Andes and the Rio Manu. It is similar to the hilly forests, but contains different soil and trees only 20-30m high. The canopy is uneven and much of the upland forest is deciduous, implying that this forest type should experience the greatest amount of leaf loss in the dry season.

It is not readily apparent that upland and floodplain forest types found in the Manu area are valid in all parts of Amazon, and from studying images of the Manaus area, hilly regions appear to be distinguishable from the combination upland/floodplain forest type (i.e. the forest type).

In the floodplain forest surrounding the rivers, regular flooding damage occurs and therefore, many stages of forest succession can be found. For example, areas far from the rivers and flooding are the most mature, with a very homogeneous, closed canopy and an average height of 50m. The understory of this mature forest contains a homogeneous growth of palms. As one approaches the rivers, however, a less regular forest can be found. Stands of almost pure *Heliconia* banana plants from 2-3m high signal the first stage of regrowth. In areas where severe flooding has killed everything, the forest is very disturbed with a dense cover of *liana* vines. These areas generate a strong L-band response. Other areas known as Aguajales are characterized by stands of *Mauritia* palms. These palm stands range from very wet to dry and also generate a strong L-band response.

CLASSIFICATION METHOD

Mean Backscatter and Texture Image Generation

Both mean backscatter (σ^0) and the standard deviation of texture were used as features for classification of vegetation types. Backscatter images provided in a full resolution (12.5m by 12.5m pixel spacing) 16 bit amplitude format by NASDA were converted first to full resolution byte images and then averaged down using 8x8 pixel boxes to produce low resolution (100m by 100m pixel spacing) byte amplitude images. The following equation from [5], [6] was used to calculate the standard deviation of the texture:

$$\sigma_T^2 = \frac{N(\sigma_p/\mu_p)^2 - 1}{N+1} \left(11 + \frac{1}{\text{SNR}} \right)^2$$

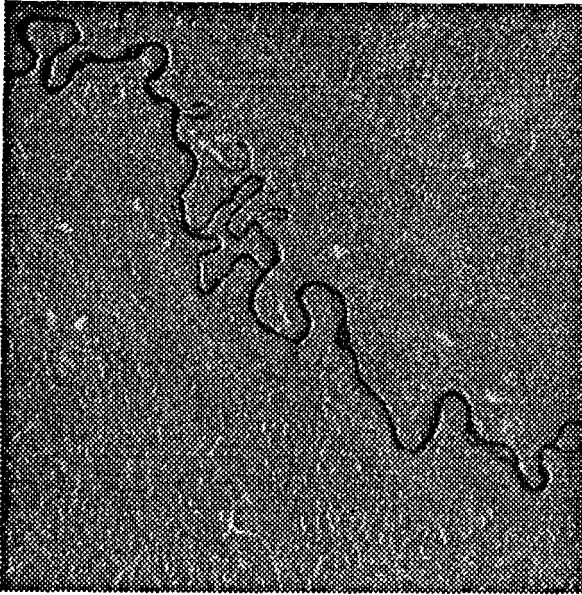


Figure 1. Portion of Backscatter Image ID c0064b26 showing Rio Madre de Dios

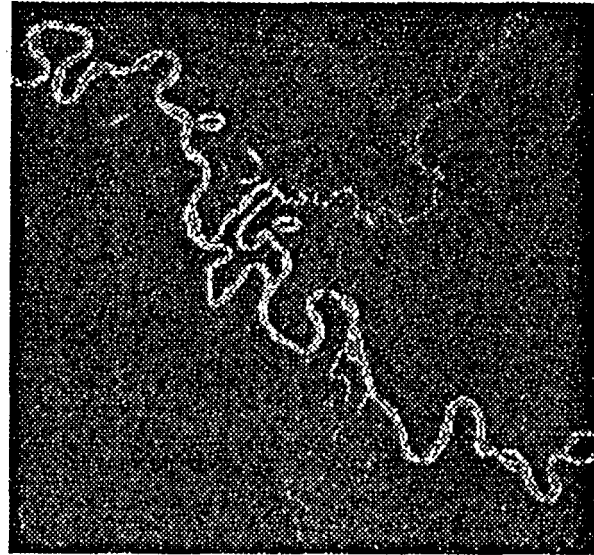


Figure 2. Texture Map for to Figure 1

where σ_p is the standard deviation of the pixel intensities over some area and μ_p is the mean pixel intensity. In practice, σ_p and μ_p for this study were calculated using 8x8 pixel boxes from full resolution backscatter images so that the resulting texture image pixel size was the same as that of the low resolution backscatter image.

Both mean backscatter and texture were essential measurements for this classifier. Mean backscatter separated flooded forest, open water, clear-cuts, and urban areas. Texture distinguished more subtle features, such as rivers hidden beneath the rain forest canopy. Furthermore, since texture is essentially a ratio of standard deviation over mean, it was found to be unaffected by first-order calibration errors.

J-ERS-1 Image Correction

In order to classify a J-ERS-1 σ^0 image, it must first be calibrated [4]. However, some residual calibration errors may remain which can cause the classifier to break down. For example, data sets available showed cross-track calibration errors appearing as dark or bright vertical bands [7] resulting in unclassified or misclassified forests. In order to minimize this problem, prior to classification images were corrected with respect to the original training image by averaging the backscatter for a number of vertical and horizontal image strips and then obtaining a scaling factor for each strip defined as

$$\text{scaling factor} = \frac{\mu_{\text{Training Image}}}{\mu_{\text{Correction Strip}}}$$

to be applied to every pixel in that strip.

Since the texture measurement is essentially a ratio of standard deviation over mean, first-order calibration errors cancel, having no effect on the texture. The most significant error source for the texture measure is the SNR estimate. Early attempts to scale the texture images with respect to a training image did more harm than good, so all texture images were left untouched.

River Masking / image Processing

in J-ERS-1 SAR data open water appears dark, with a very low σ^0 that is strongly affected by the noise floor. In addition, the texture changes depending upon whether we are in the center of a lake or near a river bank. As a

result of these properties, it was found that the best way to classify open water was by applying a region growing operation to the σ^0 data. In this method, we find regions of connected dark pixels and call them water. Since low vegetation also appears dark, a threshold is applied to distinguish between the two classes.

Our first attempts at classifying J-ERS-1 SAR image data resulted in many false alarms in hilly regions. The backscatter variations associated with the changing slopes of the terrain was often mistaken for water by the classifier. To correct this problem, image processing operations were performed to isolate rivers in hilly regions. This involved convolution with a 17x17 Difference of Gaussian edge detecting filter, global thresholding, and region growing of the resulting river areas.

Both of these operations occur before the Bayesian maximum-likelihood classification, creating image masks which denote certain pixels as water or low vegetation. These masks reduce the amount of confusion by effectively removing potentially troublesome pixels through the use of simple rules which are not based on probability measures. The information contained within these masks is ultimately combined with the results of the Bayesian classification through a series of logical rules.

Maximum-likelihood Classification

The classification scheme implemented in this algorithm is based on a supervised Bayesian maximum-likelihood classifier. Essential components of such a classifier are as follows:

- (1) A feature vector containing the measurements of interest
- (2) Training patterns representing distinct classes
- (3) Statistical models of these classes
- (4) Decision rules to determine which class the feature vector is most likely to belong.

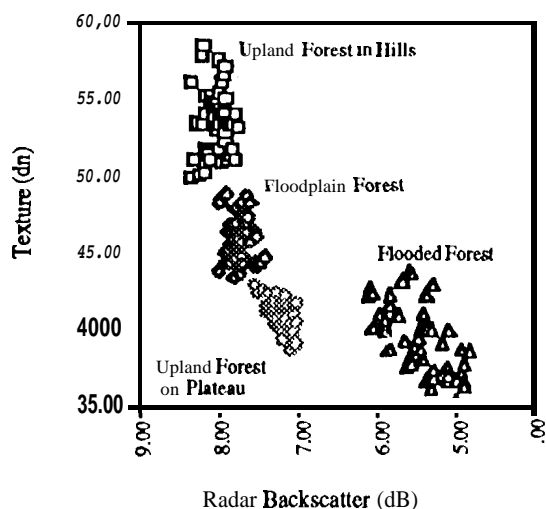


Figure 3. Training patterns created by averaging 15x15 boxes around a given pixel

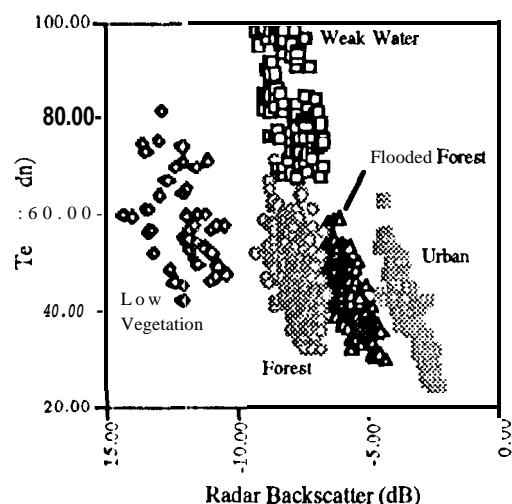


Figure 4. Training patterns created by averaging 3x3 boxes around a given pixel

For classification of J-ERS-1 images of the Amazon, the feature vector was comprised of two components, backscatter (σ^0) and the texture measurement discussed earlier. Each pixel in a J-ERS-1 image to be classified is represented by these two measurements.

By examining the available J-ERS-1 SAR data and ground measurements made in Manu National Park, seven vegetation classes were distinguished:

- (1) Upland forest
- (2) Floodplain forest
- (3) Flooded forest
- (4) Low vegetation, such as clear-cut
- (5) Water
- (6) Urban areas
- (7) Unknown.

Pixel Box Size - Forest Class	σ^0 mean	texture mean	σ^0 variance	texture variance	covariance
15x15- Upland (hills)	- 8 . 0	0.53	0 . 0 2	0.0004	0.00004
15x15- Upland (plateaus)	- 7 . 2	0.41	0.02	0.0008	-0.00064
15x15- Floodplain	- 7 . 7	0.46	0.02	0.0002	-0.00038
15x15- Flooded	- 5 . 5	0.39	0.13	0.0048	-0.00490
3x3 -Forest	- 7 . 6	0.46	0.26	0.0057	-0.01899
3x3 -Flooded	- 5 . 7	0.43	0.33	0.0045	-0.02866
3x3 -Low Vegetation	- 12 . 0	0.58	0.94	0.0085	-0.03597
3x3 -Week Water	- 7 . 9	0.82	0.45	0.0088	-0.03354
3x3 -Urbanarea	- 3 . 4	0.39	0.36	0.0077	-0.04657

Table 1. Statistics for the Training Patterns

Once these were chosen, training patterns were created to provide a model of each class. Since no one image contained sufficient quantities of every class, the training patterns were extracted from several images, using box sizes of 3x3 or 15x15 pixels for the calculations. The patterns for floodplain forest, upland forest, and water were tabulated from data taken of Manu National Park, Flooded forest and urban areas were found in sufficient quantity in images of Manaus, Brazil. Finally, low vegetation in the form of extensive clear-cuts was found in an image of Sena Madureira, Brazil.

Bivariate Gaussian distributions were chosen to model each training pattern. In order to calculate these distributions, the mean, variance, and covariance of both σ^0 and texture were calculated and are listed in Table 1. For the purposes of decision making, the *a priori* probability y of each class occurrence was assumed to be equal.

Classifying Hill Forest

Once the Bayesian classification was completed the classifier searched for areas to be classified as hill forest. First, 3x3 pixel box averages of backscatter and texture around each pixel were passed through an initial threshold filter to generate a first data set of hill forest candidate pixels. This first pass through the scene served to exclude much of the flooded forest, water and low vegetation using a box size capable of resolving small features. Then, for a second pass, standard deviations of DN (backscatter image pixel data number) values for 15x15 boxes around the hill forest candidate pixels were passed through another thresholding operation generating a second data set containing updated hill forest candidate pixels. This pass eliminated much of the upland and floodplain forest regions. A third pass through the scene involved passing the standard deviations of DN values for 21x21 pixel

Class	3x3 σ^0 mean (pass 1)	3x3 texture mean (pass 1)	15x15 DN std. dev (pass 2)	21x21 DN std. dev (pass 3)
Upland & Floodplain Forest	- 7 . 4	0.44	10.8	10.5
Flooded Forest	- 4 . 6	0.41	29.9	
Low Vegetation	- 9 . 0	0.49	16.7	14.8
Water	- 7 .	0.85	20.6	17.0
Hill Forest	-7.2	0.46	15.6	15.5

Table 2. Box statistics for Hill Forest training image(c0171a19)

boxes minus any pixels previously classified as flooded forest around the updated candidate pixels through yet another threshold filter in an attempt to eliminate some of the residual hill misclassifications from the previous passes, particularly on the borders of flooded forest regions or rivers with other forest types. The result was the final hill forest classification. Table 2 suggests that threshold operations can be effective to perform the hill forest classification as described above.

The Final Step

An ambiguity of great concern involved the upland and floodplain forest types. Since the training patterns were created from an image of the Western Amazon where ground observations were made, accurate forest classifications for the Manu images can be expected. Furthermore, it is assumed that the forests from the Western Amazon will generalize throughout the entire rain forest. However, some suspicious forest classifications have appeared throughout scenes near Manaus (e.g., upland forests occurring near flooding rivers while floodplain forest occurs further away). Two factors may be contributing to this problem:

- (1) the existing training patterns lack the necessary information to generalize correctly throughout the Amazon
- (2) very different forest types exist near Manaus which require entirely new training patterns or rules to correctly distinguish them.

This forest type ambiguity led to the employment of a final step consisting of grouping the Upland and Floodplain Forest classes into a single forest class. In addition, the brightness of forest and hill forest pixels were made proportional to the backscatter to show features in these regions which could contribute to a better understanding of the nature of the terrain from the final classified image.

Generalizing the Classifier

In creating a classifier which operates on only one or two images, it is conceivable to account for most image oddities directly within the context of the classifier code. However, when faced with the prospect of producing vegetation maps for hundreds or thousands of images, there must be some way for the algorithm to adjust to a wide variety of circumstances. In our classifier, this is handled by a set of user-controlled options. At the present time, the following options are in place:

- (1) Toggle on or off averaging filters which smooth the forest and low vegetation classifications.
- (2) Permit pixels to be classified as urban. This is necessary since highly disturbed forest may look identical to some urban areas.
- (3) Permit pixels to be classified as hill forest. Selecting this option only for scenes with hills present will avoid hill forest misclassification.
- (4) Allow the user to manually set the σ^0 threshold between water and low vegetation.
- (5) Allow the user to exert greater control over the J-ERS-1 image correction process mentioned earlier.

CLASSIFICATION RESULTS

The classifier was first tested on the Manu National Park training image. Several noteworthy features were immediately apparent in the vegetation map. First, irregular yellow spots represented areas of bright L-band response, such as palm stands, inundated areas, and regions of highly disturbed forest. Several small rivers which were barely discernible in the original image showed a high texture, and therefore were easily distinguished by the classifier. Three examples are the Rio Blanco which empties from the southwest into the Rio Madre de Dies, and the Rio Los Amigos and Rio El Amiguillo in the hills north of the Rio Madre de Dies. The floodplain forest can be seen surrounding the Rio Madre de Dies and the small rivers in the hills.

Looking at a vegetation map of a J-ERS-1 SAR image taken near Manaus, Brazil, in July 1993, we saw additional features that can be discerned by the classifier. The effectiveness of the river masking procedure was evident, as displayed by the algorithm's ability to accurately classify large expanses of open water as well as follow narrow, convoluted waterways and inlets. Large tracts of flooded forest were detected in addition to inundation effects

near small rivers. Clear cutting was also prevalent, and some areas of low vegetation were detected near river boundaries.

Not everything was perfect, however. Rather large occurrences of the Unknown class appeared at the boundaries between water and flooded forest. This can be attributed to the classifier attempting to average two very dissimilar pixel types and getting caught somewhere in between the two vegetation classes. Some of the clear-cuts also contained erroneous spots of water. These misclassifications were the result of darker than usual clear-cuts combined with an imperfect thresholding operation during the river masking procedure. Some of this can be remedied with the user options, but often at the expense of smaller waterways being mislabeled as low vegetation. There is just not enough separation between these classes in the data.

Regarding the hill forest classification, particularly troublesome areas appeared at the boundaries of flooded forest with forest classes. Some misclassification may remain in the final product, however since the brightness of the hill forest class is proportional to the backscatter, it is possible in many cases to pick out this form of misclassification by visual inspection.

An upper bound on the classifier performance (hill forest and urban regions not included) was estimated by calculating the classification accuracy in areas of the Manu training image for which ground truth was available. In Table 3, the "# ground truth pixels" column represents the number of pixels known, from the ground truth data, to belong to a specific class while the "# matching pixels" column shows how many of those pixels were actually assigned to the correct class in the final classification image. The "upper bound on performance" column is simply the percentage of correctly classified pixels. The water measurements were made on small rivers hidden under

Class	# ground truth pixels	# matching pixels	upper bound on performance
Forest	300	287	96%
Flooded Forest	150	143	95%
Low Vegetation	50	49	98%
Water	100	82	82%

Table 3. Upper bound on the classifier performance

the forest canopy, so for expanses of open water the performance of the classifier is expected to be better than what is shown here.

Perhaps more interesting than looking at the classification of one scene is comparing a sequence of vegetation maps created from data taken over an entire year. As the season shifted from dry to rainy, a definite seasonal effect was observed. Manu images taken in March showed a few large flooded forest regions that did not appear elsewhere throughout the year. These spots were regions in the original image which generated high L-band responses and only appeared flooded during the height of the wet season. More likely than not, these were spots that had experienced recent flooding damage or were sensitive palms which grew leaves only during the wettest months.

CONCLUSIONS

An algorithm has been presented that classifies vegetation types present in J-ERS-1 images of the Amazon Rain Forest. Radar backscatter and the standard deviation of texture are measurements used to distinguish the vegetation types. At the heart of the algorithm is a supervised, Bayesian maximum-likelihood classification capable of differentiating the following classes: Forest, Flooded Forest, Low Vegetation (clear-cut areas), Urban, and Water. A series of thresholding operations are employed to differentiate a class denominated Hill Forest. Image processing techniques such as edge-detection, thresholding, and region growing are implemented to reduce confusion by masking some water and low vegetation pixels before the Bayesian classification is actually run. An image scaling operation is also performed to reduce the effect of cross-track calibration errors. Realizing the difficulty in trying to create a generalized algorithm which can deal with hundreds of images, a set of user options to tailor the classification rules is under continual development.

So far, 9 images of Manu, 18 images of Manaus, and 6 images of Sena Madureira have been classified. Results indicate an excellent ability to classify water in all forms, including open water and rivers hidden beneath the rain forest canopy. Flooded forest, low vegetation, hill forest and urban areas are also distinguished with only occasional confusion. Upland and floodplain forest are classified accurately in images of Manu, but there appears to be some difficulty in generalizing these two forest classes beyond the Western Amazon, so they have been combined into a single forest class.

The ultimate goals of this classifier are to track deforestation, detect seasonal effects such as flooding, and accurately map the forest types throughout the Amazon. So far, we are well on our way to achieving all three goals. Clear cuts have been accurately detected in images of Manaus and Sena Madureira, and our vegetation maps have shown the ebb and flow of flood waters in seasonal sequences taken over Manu and Manaus. Evaluation of the classifiers performance could be enhanced by increased availability of ground truth data, however the results are very promising thus far, with our algorithm capable of classifying to a high degree of accuracy images ranging from the Western Amazon to Brazil.

ACKNOWLEDGMENTS




The authors acknowledge the contributions from Masanobu Shimada of NASDA, who made the data available. For the ground deployment to Manu National Park, we thank Reiner Zimmermann, Flare Oren, Sharon Billings, Viviana Horna, and John Terbourgh.

The research described in this paper was carried out by the Jet Propulsion Laboratory, California Institute of Technology, under a contract with the National Aeronautics and Space Administration.

REFERENCES

- [1] Shimada, M., "J-ERS-1 SAR Calibration and Validation", presented at the CEOS SAR Calibration Workshop, Noordwijk, The Netherlands, September 1993.
- [2] Hara, Y. and One, M., "Analysis of J-ERS-1 SAR Imagery", Proceedings IGARSS '93, pp. 1191-1193.
- [3] Yamagata, Y. and Yasuoka, Y., "Classification of Wetland Vegetation by Texture Analysis Methods Using ERS-1 and J-ERS-1 Images", Proceedings IGARSS '93, pp. 1614-1616.
- [4] Freeman, A., Alves, M., and Williams, J., "Calibration Results for J-ERS-1 SAR Data produced by the Alaska SAR Facility", Proceedings IGARSS '93, pp. 965-967.
- [5] Ulaby, F., Moore, R., and Fung, A., *Microwave Remote Sensing, Volume 3, USA*, Addison-Wesley, 1986
- [6] P. H. Swain, *Remote Sensing, the Quantitative Approach*, United States of America: McGraw-Hill, Inc., 1978.
- [7] B. Chapman, M. Alves, A. Freeman, *Validation and Calibration of J-ERS-1 SAR Imagery*, Proceedings of the J-ERS-1 Results Reporting Meeting, 1995.

Classification from J-ERS-1
Manaus, Brazil (October, 1993)

-  Forest
-  Hill Forest
-  Flooded Forest
- Low Vegetation
- Water
- Urban

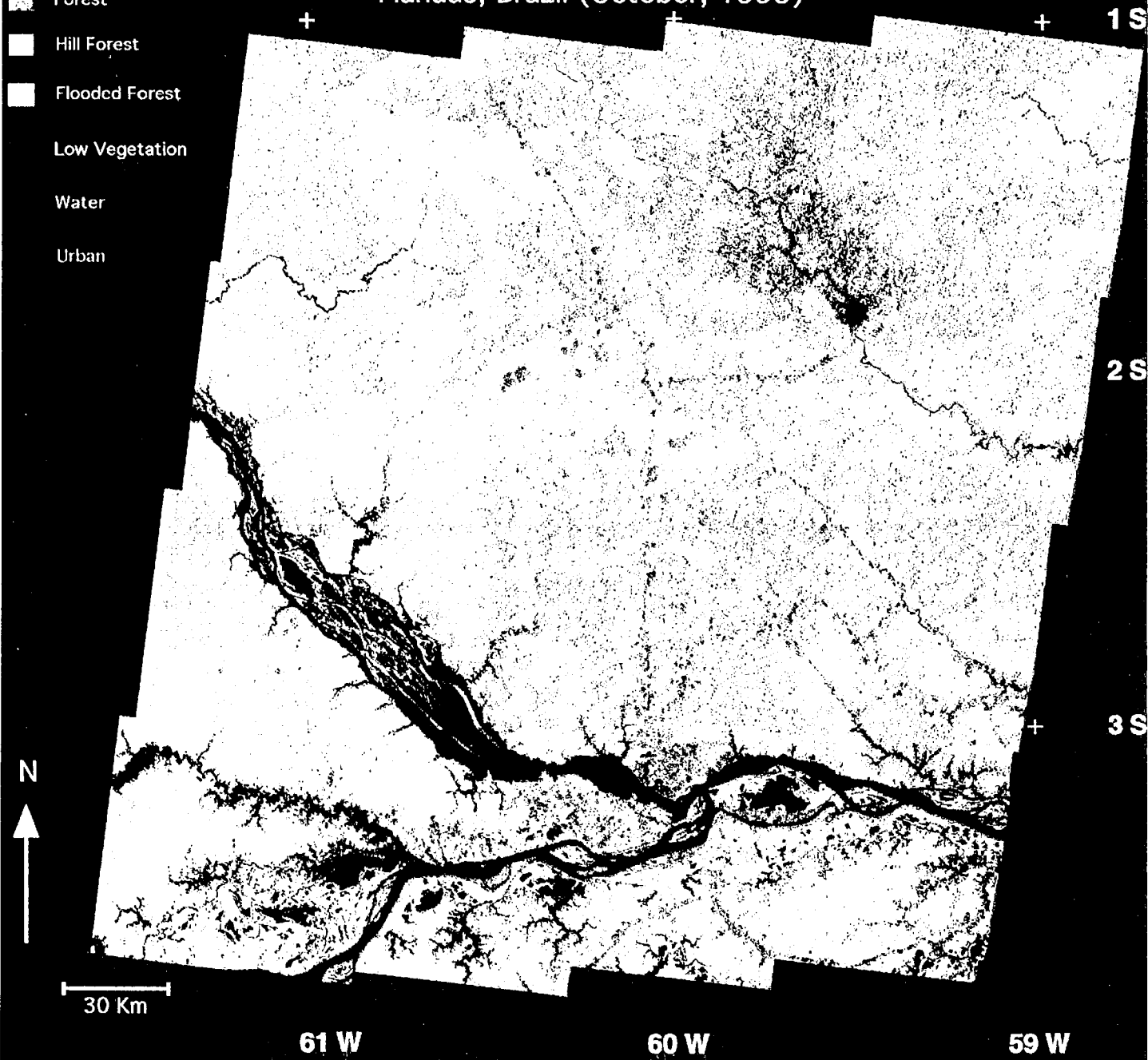


Plate 1. This classification map was obtained from 16 J-IRS-1 images that were acquired in October, 1993. The data was classified by examining the backscatter values of the low resolution data (200 meter) and the corresponding texture values as described in the text. The Rio Negro, the northernmost wide river in the image, meets the Rio Solimões just South of the urban area of Manaus. At this point, the river is known as the Amazon as it flows eastward to the Atlantic. One hundred kilometers North of Manaus is a reservoir that has flooded the surrounding rain forest.